Synthesis and Characterization of Nanoreactors within Polymeric Nanotemplates

M. McTaggart[*], M. Groves[**], C. Malardier-Jugroot[*,+] and M. Jugroot[***]

[*]Chemistry and Chemical Engineering Department, Royal Military College of Canada, Kigston, ON, Canada, matt.mctaggart@rmc.ca
[**]Physics Department, Aarhus University, Aarhus, Denmark, groves@phys.au.dk
[***] Mechanical and Aerospace Engineering Department, Royal Military College of Canada, Kigston, ON, Canada, jugroot-m@rmc.ca
[+]cecile.malardier-jugroot@rmc.ca

ABSTRACT

The paper will present a novel method for the synthesis of metal nanoclusters with diameters < 3nm within an amphiphilic nanotube template without the use of a reducing agent. This environmentally friendly synthesis occurs at neutral pH in aqueous environment within the confinement of a polymeric nanotube with an internal diameter of 2.8 nm. The synthesis and characterization of Au and Pt nanoclusters using UV-Vis spectroscopy and transmission electron microscopy will be described. Characterization results will be extensively compared to ab initio molecular simulations of the metal clusters and its interactions under confinement.

Keywords: nanoclusters, nanotube, confinement, green chemistry

1 INTRODUCTION

The most efficient catalysts have been developed and optimized by living systems [1,2]. Indeed, in vivo enzymatic action is several orders of magnitude more efficient than the same reaction under inorganic catalysis. However, the rate of reaction and equilibrium interactions are considerably reduced when the biological systems are studied in vitro [3-5]. The increase in the rate of reaction in cellular environments was attributed to two complementary effects: the reduced diffusion rate of the molecules in crowded environments and the increase in thermodynamic activities, phenomenon is largely attributed to the effect of confinement or macromolecular crowding present in the cell [4]. Confinement can also be observed in an aqueous solution containing surfactants. In fact amphiphilic copolymers can self-assemble into well-defined ordered structures such as micelles, nanotubes, vesicles; geometries and shapes of a given copolymer can be precisely controlled by their solvent affinity. Hollow nano-architectures with a hydrophobic inner cavity induces confinement for molecules solubilized inside the polymeric template obtained by self-assembly.

A controlled environment for the study of confinement allows the unique synthesis of metal nanoparticles from metal salts without reducing agents in water at room temperature and neutral pH. This new environmentally friendly method produces catalytically active platinum nanoparticles with diameters under 3nm and accordingly large surface area.

2 METHOD

Four samples of hydrophobic metal salts (98% PtCl2 and 99.9% AuCl, both purchased from Sigma-Aldrich) were mixed into 1%wt poly(styrene-alt-maleic anhydride) (350,000 mw avg, Sigma-Aldrich) in 3mL of water neutralized to pH 7 with NaOH such that the total metal content should have a 1:1 molar ratio with the SMA monomers.

Samples 1 and 2 contained PtCl2 and AuCl, respectively. Sample 3 was prepared by adding a mix of equal parts PtCl2 and AuCl to the SMA solution. Sample 4 also contained equal parts PtCl2 and AuCl, but each metal was first introduced to individual 1.5 mL amounts of SMA solution and subsequently mixed together after one day. All samples were sonicated for one hour after the metal salts were added and stored in a dark, room temperature environment for the duration of the measurement period.

UV/vis spectra were measured in a 1 mm path-length quartz cuvette with an Agilent 8453 PDA spectrometer. Data was captured by ChemStation software v.B.04.02. Spectra were taken once daily over 19 days save for day 4 and 11, and again on day 98.

Molecular simulations were completed with Gaussian 09 software [6]. All molecular models were optimized using DFT-B3PW91with lanl2dz basis set [7-9].

Transmission electron microscopy was performed at the Canadian Centre for Electron Microscopy at McMaster University. Aqueous solutions of the PtCl2 reduced in 1wt% SMA was deposited onto a copper TEM grid and left to dry in air at room temperature. Images were recorded using a FEI Titan 804300 LB TEM.

3 RESULTS

3.1 Sample 1: PtCl2/SMA

Platinum nanocrystals have no plasmon band in the visible range but do produce a characteristsic peak at 215nm in the UV range. Unfortunately, that peak is

obfuscated in this system by SMA's broad UV absorbance. Platinum reduction and nanocrystal formation can be monitored qualitatively by the solution's colour change from yellow to brown to nearly black [10], a change seen in Figure 1 as the dissipation of the shoulder at 430 nm. The colour of sample 1 evolved slowly over the nineteen day measurement period from yellow to yellow-brown.

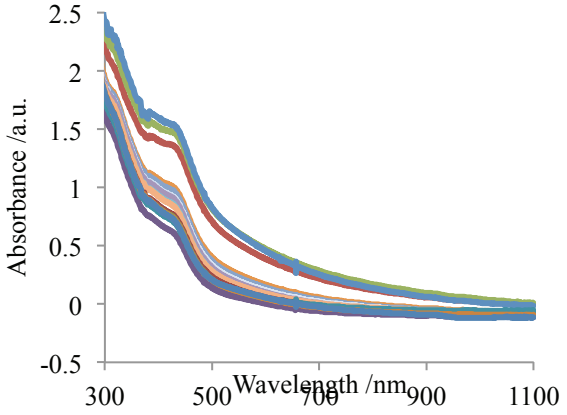

Figure 1: UV/vis spectra of sample 1 (PtCl2/SMA). Shoulder peak centred at 430 nm; absorbance intensity diminishes over time.

Slow reaction kinetics of platinum reduction in SMA would suggest that it is, at least initially, dependent on a relatively rare reaction event. Simulation of a platinum atom placed equidistant from styrene and oxygen groups present on the SMA monomer shows a thermodynamic preference for the hydrophobic group. In fact the optimal geometry was found when platinum substituted onto the styrene ring with a bonding energy of 215.6 kJ·mol^{-1}. Subsequent platinum atoms bond to the first with energy on the same order.

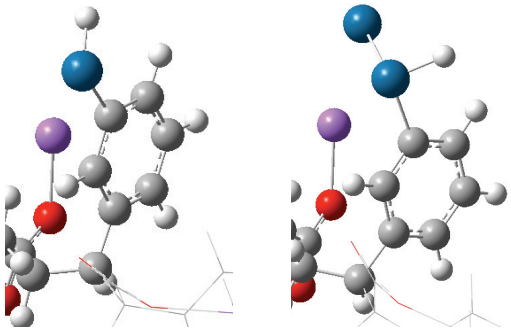

Figure 2: DFT-B3PW91/lanl2DZ optimized Pt/ SMA trimer model system, cropped to area of interest for clarity.

Platinum reduction and sequestration within the hydrophobic core of SMA nanotubes has been confirmed by TEM imaging, shown in Figure 3. Indeed no platinum was observed outside of the SMA matrix, nor were any found with a diameter greater than 3 nm. The Pt/SMA system creates a nanoreactor capable of catalyzing organic reactions under confinement without the need for organic solvents. Pyrrole polymerization, a reaction known to spontaneously occur in 1wt% SMA [11], was increased three times by the presence of platinum nanocrystals (results not shown).

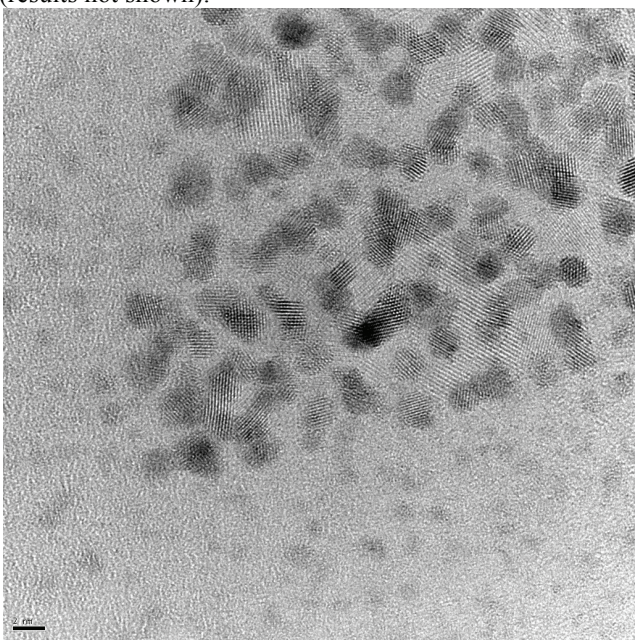

Figure 3: TEM image of platinum nanocrystals reduced and held within SMA nanotubes. Scale bar is 2nm.

3.2 Sample 2: AuCl/SMA

Unlike platinum, colloidal gold does have a visible plasmon band that is known to vary in wavelength between 520 and 580nm in proportion to size, Figure 4. The general shape of gold nanoparticles can also be determined since each dimension will produce the spectral band associated with its width. The single peak observed here indicates that the demonstrated method produces nominally spherical nanocrystals.

The diameter of spherical gold colloids in water can be determined by the folowing formula derived from mean free path adjusted Mie's theory:

$$d = \frac{\ln\left(\frac{\lambda_{spr} - \lambda_0}{L_1}\right)}{L_2} \quad (1)$$

Where the theoretical fit parameters λ_0 = 512, L_1 = 6.53 and L_2 = 0.0216 [12]. As shown in Figure 4, the peak produced by nanoparticles in sample 2 are centered at 547nm. The peak wavelength does not tend to shift as it grows, indicating that size is relatively consistent and stable. In accordance with Equation 1, gold nanoparticles produced by this method are 77.7nm +/- 3% in diameter. An alternative equation based on the ratio of absorbance at the surface plasmon peak to that at 450nm and experimentally derived fit paramers gives a diameter of 76nm, within the 3% margin of error [12].

If indeed the gold nanoparticles are 77nm in diameter, then they are clearly not bound within the 2.8nm inner diameter of SMA nanotubes and likely form by a separate mechanism from that responsible for platinum. Simulations of an AuCl molecule placed equidistant from SMA's styrene and carboxyl groups demonstrate the gold atom's greater affinity for the hydrophilic exterior group, Figure 5.

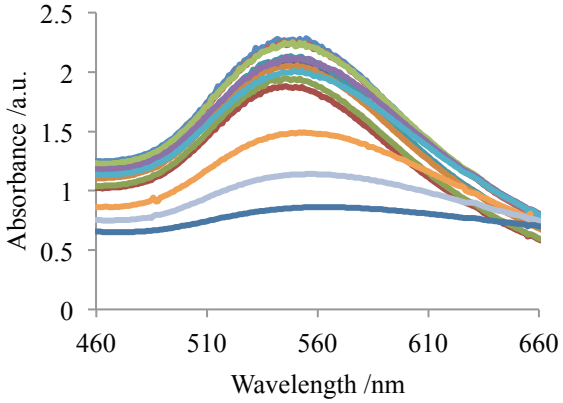

Figure 4: UV/vis spectraof sample 2 (AuCl/SMA). Peak centred at 547nm; intensity increases over first 9 days, then settles.

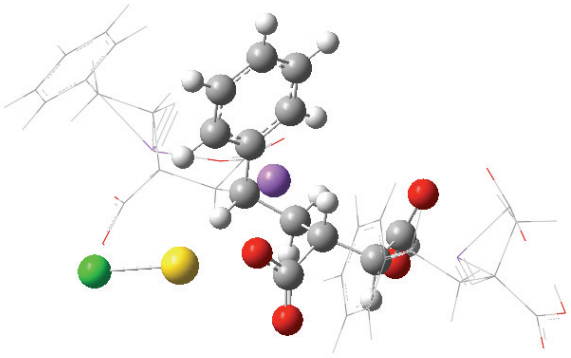

Figure 5: DFT-B3PW91/lanl2DZ optimized AuCl/SMA trimer model system.

It should be noted that the above equations were derived for free gold colloids in water and confirmed against to preparations of the same. Since the determination of diameter by these equations is highly sensitive to the surface plasmon peak wavelength and it is yet unknown whether and to what degree the SMA surface affect the dielectric environment on the gold surface, TEM imges are needed to confirm the diameter.

3.3 Sample 3: PtCl2:AuCl/SMA

The UV/vis spectra of sample 3 show the growth of a single, low-intensity peak centred at 554nm, Figure 6. A red shifted and reduced peak was reported by Miner et al [13] to represent a 75:25 alloy of gold and platinum. The red shift is relatively small in the present case, possibly indicating an even greater ratio of gold to platinum.

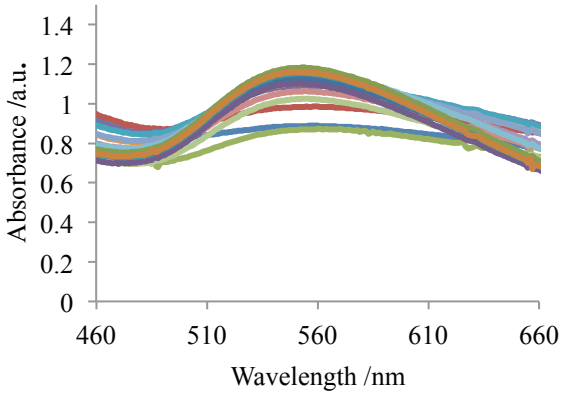

Figure 6: UV/vis specra of sample 3. Peak centred at 554 nm; intensity rises over time.

Sample 3 is notably blacker than sample 2, as would be expected for a colloid with platinum surface features. The addition of gold nanocrystals to platinum chloride solution is known to seed crystal formation in a core-shell arrangement under conditions similar to those described here [14]. Where gold reduction and crystalization kinetics are faster than platinum, the gold nanocrystal cores catalyze the formation of polycrystaline platinum nanowires on its surface that can, with a sufficient Pt:Au ratio, coat the entire gold surface.

3.4 Sample 4: PtCl2/SMA:AuCl/SMA

In sharp contrast to sample 3, when the metal salts were mixed with SMA in solution prior to being mixed together gold and platinum nanocrystal formation remains largely independent, as evidenced by the growth of the gold peak at 547 nm and the platinum shoulder at 430 nm in Figure 7.

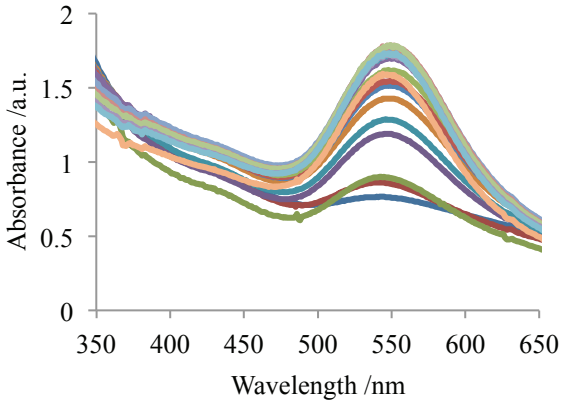

CTSI-Cleantech 2014, www.ct-si.org, ISBN 978-1-4822-5819-6

Figure 7: UV/Vis spectra of sample 4. Peak centred at 547nm; intensity rises with time.

Since the platinum reduction reaction is thought to be bound within the hydrophobic core of the SMA nanoutbes while gold crystal formation may occur on the hydrophilic surface, the initial partition of the metals into these separate phases may hinder the creation of bimetallic particles.

When the final spectra of all four samples are compared directly, as in Figure 9, the congruence of sample 2 and 4 is immediately apparent. Also, the shoulder in the platinum spectrum remains suggesting that the reaction in sample 1 had not gone to completion. Finally, the red shift and intensity drop associated with a gold/platinum surface is clearly seen in sample 3 and , to a smaller degree, in sample 4 once the individual contributions of platinum and gold nanocrystals are removed.

Figure 9 also shows the UV/vis spectra of the samples after 98 days. While the general trends remain, there is a blue shift in the peaks from 547 to 540 nm (Au) and 554 to 545 nm (AuPt). By Equation 1, the Au shift would indicate a 10 nm decrease in nanocrystal diameter. Unstable nanocrystals tend to aggregate rather than shrink, suggesting that the SMA coating has a significant effect on light transmission.

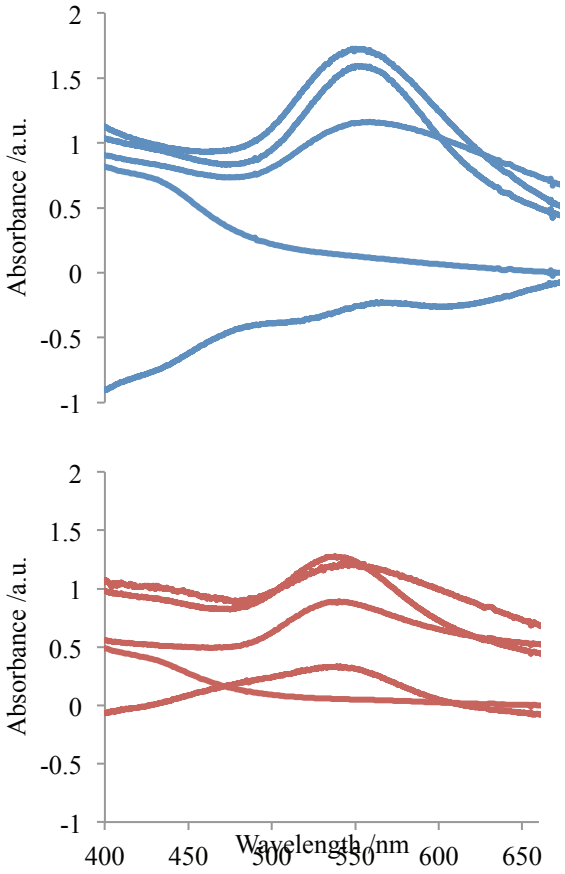

Figure 9: UV/Vis results on day 19 (above) and 98 (below). Pt: solid; Au: long dash; AuPt: dotted; Au & Pt: short dash; Au&Pt –Au –Pt: dash-dot.

4 CONCLUSION AND FUTURE STUDIES

This study demonstrates a new, facile, and ecologically sound method for the production of < 3 nm platinum crystals within the hydrophobic core of SMA nanostructures. Gold was also shown to autoreduce and form nanocrystals but at a larger diameter and by an alternate mechanism. Systems that contain both metals may form an alloy or core-shell nanoparticle, though only if simultaneously introduced into the polymer matrix.

Simulation and experimental efforts are ongoing to determine the mechanisms of crystal formation, specifically the role of confinement on platinum reduction. Further TEM experiments will show the diameter and, in the case of Au/Pt systems, surface structures of gold nanoparticles produced by this method. TEM imaging will also be used to determine the optimal conditions for control of nanocrystal size, shape, and number. The success of pyrrole polymerization shows that otherwise unfavourable reactions will occur within the confined organic phase of the Pt/SMA nanoreactor. Other reactions will be tested and reaction rates benchmarked.

REFERENCES

[1] F.H. Arnold, Chem. Eng. Sci., 51(23), 5091-5102, 1996.

[2] R.A. Gross et al., Chem. Rev., 101, 2097-2124, 2001.

[3] A.P. Milton, J. Cell Sci., 119, 14, 2006.

[4] R.J. Ellis, Trends in Biochem. Sci., 26, 10, 2001.

[5] A. P. Minton, J. Biol. Chem., 276(14), 10577-10580, 2001.

[6] Gaussian 09, Revision B.01, Frisch, M. J. et al. Gaussian, Inc., Wallingford CT, 2009.

[7] Becke, A. D. J. Chem. Phys. 98, 5648-52, 1993.

[8] Dunning Jr., T.H., Hay, P.J., in *Modern Theoretical Chemistry*, Ed. H. F. Schaefer III, Vol. 3 (Plenum, New York, 1976) 1-28.

[9] Hay, P.J., Wadt, W.R., J. Chem. Phys., 82, 270-83, 1985.

[10] Liu, Z. et al. Mater Chem. 13, 3049-3052, 2003.

[11] Li, X., Malardier-Jugroot, C. Macromolecules. 46 (6), 2258–2266, 2013.

[12] Haiss, W. et al. Anal. Chem., , 79(11), 4215-4221, 2007.

[13] Miner, R.S., Namba, S., Turkevich, J. Proc. 7th Int Congress on Catalysis, ed. Seiyama, T., Tanabe, K.. Kodansha, Tokyo, 1981, p. 160.

[14] Ataee-Esfahani, H., Wang, L., Nemoto, Y. Yamauchi, Y. Chem. Mater, 22, 6310-6318, 2010.